Gene delivery of a single,structurally engineered Coronavirus vaccine antigen elicits SARS-CoV-2 Omicron and pan-Sarbecovirus neutralisation

Jonathan Heeney (jlh66@cam.ac.uk)
University of Cambridge https://orcid.org/0000-0003-2702-1621
Sneha Vishwanath
University of Cambridge
George Carnell
University of Cambridge https://orcid.org/0000-0001-8875-0989
Matteo Ferrari
DIOSynVax Ltd
Benedikt Asbach
University of Regensburg https://orcid.org/0000-0003-1056-8591
Martina Billmeier
University of Regensburg
Charlotte George
University of Cambridge https://orcid.org/0000-0002-6585-3288
Maria Suau Sans
University of Cambridge
Patrick Neckermann
University of Regensburg
David Peterhoff
University of Regensburg
Diego Cantoni
Viral Pseudotype Unit, Medway School of Pharmacy, University of Kent
David Wells
Liverpool John Moores University https://orcid.org/0000-0002-4531-5968
Nigel Temperton
University of Kent https://orcid.org/0000-0002-7978-3815
Simon Frost
Microsoft Health Futures

Article

Keywords:

Posted Date: January 26th, 2022

DOI: https://doi.org/10.21203/rs.3.rs-995273/v1

Gene delivery of a single, structurally engineered Coronavirus vaccine antigen elicits pan-Sarbecovirus neutralisation and protects from Delta variant challenge

DBPR

Abstract

Of the coronaviruses that have caused zoonotic spill-overs in past two decades, the diverse group of betacoronaviruses (B-CoVs) represent the greatest threats. Towards achieving broad vaccine protection from these viruses, vaccines composed of multiple antigens, each capable of eliciting broad neutralising responses across a subgroup will be required. Here we describe a novel platform for selecting immune optimized, structurally engineered antigens capable of eliciting protective responses across a group of related viruses and demonstrate proof-of-concept against the sarbecoviruses subgenus with a single antigen structure. From an array of phylogenetically informed antigen structures displaying different broad neutralising epitopes, synthetic genes expressing these were selected based on broad immune responses in BALB/C mice. Improved protection against the Delta variant was observed in K18-hACE2 mice on boosting with the lead designs of mice primed by an approved COVID-19 vaccine. Immunogenicity of the lead vaccine antigen was confirmed in guinea pigs using needleless intradermal immunisation. The broad neutralising immune profile against SARS-CoV, SARS-CoV-2, WIV16, and RaTG13 was further confirmed in rabbits with GMP manufactured DNA immunogen. Notably, sera from immunised rabbits showed potent antibody responses against Beta, Gamma, and Delta variants of concern. Here we demonstrate proof-of-concept of this Digitally Immune Optimised, Selected vaccine (DIOSvax) antigen pipeline for the *in vivo* selection of single nucleic acid-based immunogens. Such gene-based antigens can be readily delivered alone or, in combination for vaccines designed to prevent future pandemics, can be seamlessly scaled with vaccine delivery modalities such as viral vector or mRNA based vaccines.

Main

Amongst the coronaviruses of the greatest pandemic risk are the angiotensin-converting enzyme 2 (ACE-2) binding viruses of β-Coronaviruses genus [1,2]. Over the last two decades, two ACE-2 binding sarbecoviruses (a sub-genus of β-coronaviruses) have spilled over into human population causing the SARS epidemic in 2002/2003 and the current on-going SARS-CoV-2 pandemic. Bats are the reservoir of a large number of SARS-CoV-like ACE-2 binding sarbecoviruses which pose a constant threat for future spill-over into human population, and potentially new epidemics[3,4]. In addition to emergence of new ACE-2 binding viruses from zoonotic reservoirs, another concern is the emergence of variants of these viruses capable of escaping vaccine-induced immunity, a constant concern in the current on-going pandemic. As human infections increase globally during the current pandemic, the virus has continued to accrue mutations, most significantly in the spike protein[5]. An accumulating number of variants of concern (VOCs) have implications for increased transmission and escape from natural and vaccine immunity[6–9]. The N501Y asparagine to tyrosine substitution in the receptor binding domain (RBD) of the spike protein is a common feature of VOCs and is associated with increased affinity of the viral spike protein to the ACE-2 receptor and subsequent increase in transmission[10]. To date, two variants have K417N/T and E484K mutations in the RBD and are reported to escape immune responses generated by most approved vaccines[7,8]. The Delta VOC[11] is the most contagious variant reported to date, with L452R and T478K mutations in the RBD. Notably, the majority of these mutations reported in VOCs are in or around the region in RBD that interacts with ACE-2 as well as one of the regions that induce highly potent neutralising antibodies[12,13]. The continued emergence of these VOCs during the on-going COVID-19 pandemic, and the constant threat of new zoonotic spillovers of coronaviruses from animals to humans, highlights the need for next generation vaccines with broader protection from ACE-2 binding sarbecoviruses as well as the emerging VOCs. To increase the coverage

to all ACE-2 receptor using viruses of the sarbecovirus sub-genus of β-coronaviruses, we utilised a computational structure-based, RBD subunit-based vaccine strategy comparing all the known human and animal reservoir sarbecoviruses. This design was further used as backbone for designing both epitope optimised and immune re-focussed designs using available structural data for spike protein in complex with monoclonal antibodies, specifically those targeting the ACE-2 receptor binding domain (RBD), such as S309[14] and CR3022[15] that bind both SARS-CoV, and SARS-CoV-2. The nucleic acid sequence of these *in silico* designed vaccine antigens were optimised for expression in humans and synthetic genes expressing each unique antigen structure was shuttled in an expression cassette for consecutive *in vitro* and *in vivo* screens in different species to select the best-in-class immunologically optimal antigen as the vaccine candidate for nucleic acid vaccine delivery.

Sequences of spike protein of viruses belonging to the sarbecovirus lineage were compiled from NCBI virus database[16] and further pruned. The phylogenetic tree of these sequences is represented in **Fig. 1A**. Two distinct clades are observed in the tree, separating those in clade 1, which do not interact with ACE-2 receptor[1,17] from those in clade 2, which do. Clade 1 viruses share many of the sequence features of the members of clade 2 but possess deletions around the ACE-2 binding region (**Fig. S1**). An optimised core sequence (T2_13) was designed, such that each amino acid position in this sequence was optimised to be phylogenetically closer to all the sarbecoviruses represented in the phylogenetic tree in **Fig. 1A**. To further understand the importance of amino-acid composition of epitopes in generating antibody responses, we further modified T2_13 to display the epitopes of SARS-CoV for monoclonal antibodies - S309[14] (T2_14), and CR3022[15] (T2_15) and of SARS-CoV-2 for monoclonal antibody - B38[12] (T2_16). The sequence of epitopes for monoclonal antibodies - S309[14], and CR3022[15] are highly conserved across the sequences considered in this study while

the sequence of epitopes for monoclonal antibody - B38[12] is highly divergent (**Fig. 1B**). We further modified the epitope region for monoclonal antibody - B38[12] by introducing a glycosylation site on the backbone of T2_14 (T2_17) and T2_15 (T2_16). This was done to mask the divergent epitope region and enhance the presentation of the conserved epitopes to the immune system. The masking of epitopes by introducing glycans has been exploited by many viruses such as Hepatitis C Virus[18], Lassa virus[19], and Influenza[20] to escape natural immunity. To compare the immunogenicity of soluble and membrane bound RBD subunit-based vaccine, membrane bound forms of T2_13 and T2_17 (T2_13_TM and T2_17_TM respectively) were generated. The structural stability of these designs was evaluated *in-silico* using the FOLDX[21] algorithm using T2_13 as the reference model. Structural models of these vaccine antigens are represented in **Fig. 1C**.

In vivo screening in BALB/c mice was performed by immunising with different lead antigen designs (**Fig. 1D**) and assaying for cross reactive antibodies against different sarbecovirus spike proteins in a flow cytometry based cell-surface display assay. Sera taken two weeks following the second immunisation with antigen designs (T2_13 through to T2_18 and the membrane bound designs), demonstrated the binding profile of the vaccine candidates for different spike proteins (**Fig. 1E)**. As expected, sera from SARS-CoV RBD immunised mice bound strongly to both homologous SARS-CoV spike protein and closely related WIV16 spike protein in comparison to other vaccine designs, while sera from SARS-CoV-2 RBD immunised mice bound homologous SARS-CoV-2 spike protein and closely related RaTG13 spike protein in the similar range of other vaccine designs. Sera from SARS-CoV immunised mice showed binding to SARS-CoV-2 spike, though significantly less than sera from SARS-CoV-2 RBD immunised mice ($p = 0.02$) and comparable to PBS ($p > 0.05$). Across the four spike proteins, no significant differences in binding were observed for sera from mice immunised with T2_13

and sera from mice immunised with SARS-CoV-2 RBD (all $p > 0.05$), demonstrating that epitopes in this design is biased towards SARS-CoV-2 RBD. For the T2_16 design, in which the epitope region for mAb B38 was mutated to epitope region on SARS-CoV-2, binding to SARS-CoV, WIV16, and RaTG13 declined in comparison to T2_13 ($p < 0.05$) without statistical changes in binding to SARS-CoV-2. This observation is suggestive of immunodominance of this region in comparison to other sites. Matching of the epitopes of S309 and CR3022 to SARS-CoV (T2_14 and T2_15), enhanced the binding to SARS-CoV ($p < 0.05$) but not to other spike proteins. Introduction of glycosylation site in design T2_17 significantly enhanced the binding of elicited antibodies to SARS-CoV and RaTG13 ($p < 0.01$) in comparison to T2_14, but no difference was observed in T2_18 in comparison to T2_15. There was no difference between trans-membrane and non- trans-membrane bound designs. As T2_17 has either the best (or second best) median binding to the four spike proteins apart from the homologous RBD vaccine antigen, we choose T2_17 as the lead candidate for further immunological assays.

Elicitation of cross-binding antibodies by T2_17 was further confirmed by ELISA with SARS-CoV RBD and SARS-CoV-2 RBD **(Fig. 1F**), revealing robust binding antibody responses to both SARS-CoV and SARS-CoV-2 within two weeks of the second immunisation. While the T2_17 antigen elicited stronger responses against SARS-CoV, it was lower than those induced by the homologous SARS-CoV antigen, but significantly higher than SARS-CoV-2. Against SARS-CoV-2, all the three antigens – SARS-CoV RBD, SARS-CoV-2 RBD, and T2_17 generated similar binding antibody responses. Given the breadth of antibody responses induced by the T2_17 antigen, we asked if this antigen could boost and broaden the efficacy of current licensed vaccines against SARS-CoV-2 VOCs. To address this, we used homozygous K18-hACE2 transgenic mice and immunised them with $1.4x10^9$ vp of commercially available

AZD1222 (ChAdOx1 nCoV-19) and 4 weeks later boosted with either T2_17, or the licensed AZD1222 vaccine (**Fig. 1G**), while the control group received only PBS with each immunisation. Eight weeks post boost, all groups of mice were challenged with either a January 2020 isolate of SARS-CoV-2 (Victoria) or the more recent Delta variant of SARS-CoV-2 (**Fig. 1H**). Increased binding antibodies titres to both SARS-CoV and SARS-CoV-2 after boosting by either AZD1222 or T2_17 (**Fig. S2**) was observed. Significant difference in antibody titres to SARS-CoV-2 were observed four weeks after boosting with T2_17 in comparison to boosting by AZD1222 (**Fig. 1I**). Neutralising antibodies for SARS-CoV-2 and the Delta VOC were detected for all the groups, except the control group prior to challenge (**Fig. S3**). After two weeks post boost, T2_17 neutralised the Delta variant significantly better than the sera from mice boosted with AZD1222 (**Fig. 1J**). Mice from all the groups, except controls, survived and continued to gain weight following challenge with either the Victoria strain or Delta variant (**Fig. 1K**).

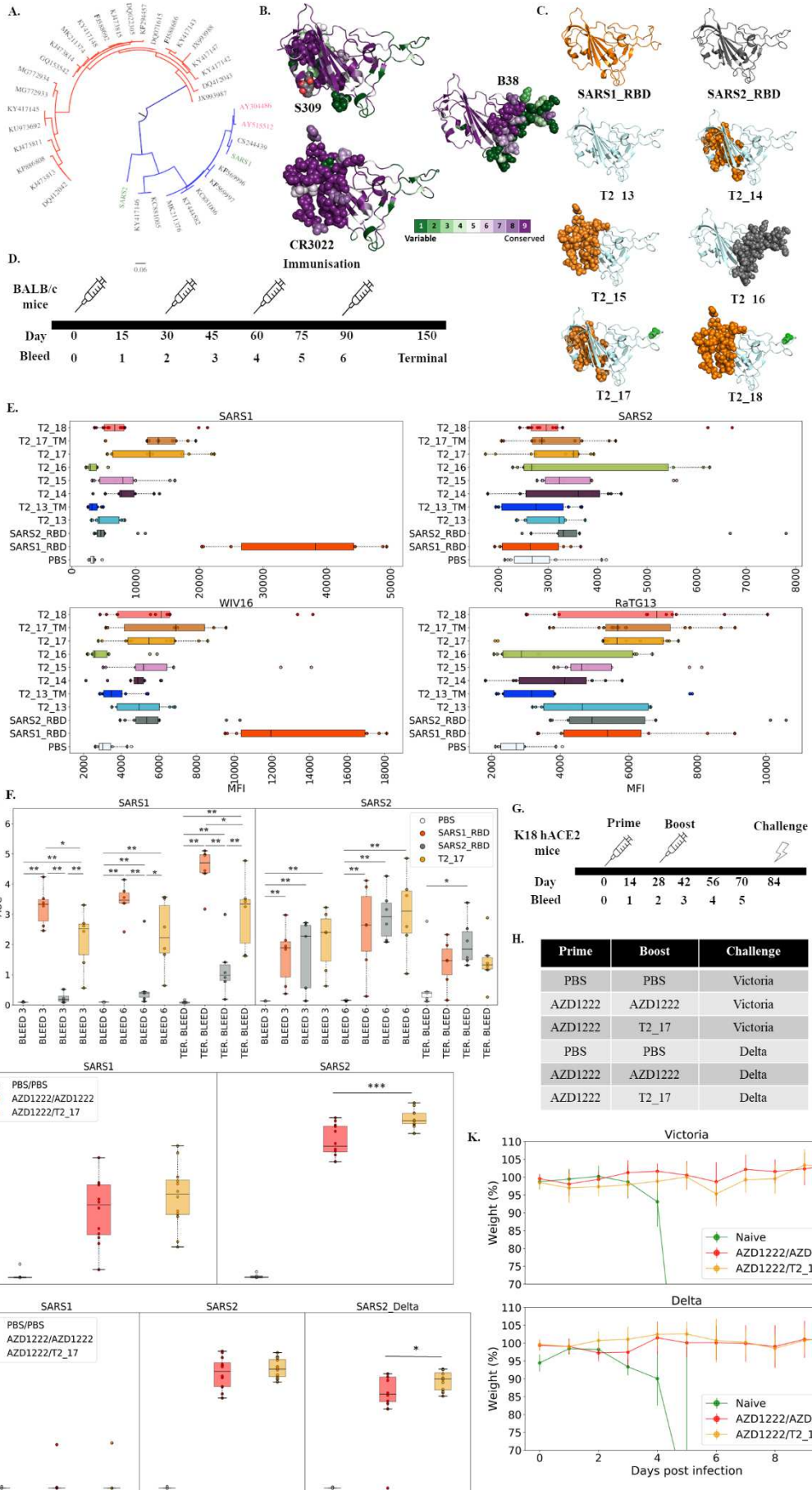

Prime	Boost	Challenge
PBS	PBS	Victoria
AZD1222	AZD1222	Victoria
AZD1222	T2_17	Victoria
PBS	PBS	Delta
AZD1222	AZD1222	Delta
AZD1222	T2_17	Delta

143

Figure 1| *In-silico* design and *in-vivo* selection of vaccine antigen candidate.

A. Phylogenetic tree generated for sarbecoviruses using protein sequence of receptor binding domain (RBD) of the spike protein. The tree was generated using IQ-Tree[22]. Human viruses are represented in green, palm civet viruses in pink and bat viruses in dark grey. The distinct two clades are coloured in red (non-ACE-2 binding) and blue (ACE-2 binding). **B**. Structural models of RBD with epitope regions highlighted as spheres. The backbone of RBD is coloured according to the CONSURF[23] score calculated using the alignment used for construction of phylogenetic tree. The figure was generated and rendered using PyMol[24] using PDB[25] id 6wps[14], 6w41[15], and 7bz5[12]. **C.** Structural representation of the different vaccine designs used in this study. The epitopes that were modified to match the wild-type SARS-CoV (coloured orange) and wild-type SARS-CoV-2 (coloured grey) are represented in spheres. Further glycosylation site modification is represented in green sphere. **D.** Immunisation and bleed schedule of BALB/c mice. Mice were immunised at interval of 30 days and bled every 15 days. **E**. FACS binding data for different vaccine designs. Sera from mice immunised with these vaccine antigens were screened for binding to SARS-CoV, SARS-CoV-2, WIV16, and RaTG13 spike proteins. The X-axis represents the mean fluorescence intensity (MFI), and the Y-axis represents all the vaccine designs considered for screening. For each mouse sera, two replicates of MFI have been reported. **F.** Elicitation of binding anti-bodies against SARS-CoV and SARS-CoV-2 by T2_17 was confirmed using ELISA, with SARS-CoV and SARS-CoV-2 RBD as control vaccine design. T2_17 generated cross-binding antibodies. The X-axis represents the vaccine designs, and the Y-axis represents the area under the curve (AUC) for ELISA binding curves. **G.** Immunisation, bleed, and challenge schedule of K18-hACE2 mice. **H.** K18-hACE2 mice were primed with AZD1222 vaccine and then boosted with either AZD1222, or T2_17 after four weeks. The mice were challenged after 8 weeks with either Victoria strain of SARS-CoV-2 or the Delta variant. **I.** Elicitation of binding antibodies against SARS-CoV and SARS-CoV-2 before challenge was confirmed using ELISA using K18-hACE2 mice sera 4 weeks post boost (bleed4). Boost by T2_17 significantly increased the binding antibody titres in comparison to boost by AZD1222. The X-axis represents the vaccine designs, and the Y-axis represents the area under the curve (AUC) for ELISA binding curves for each serum. **J.** Neutralisation of SARS-CoV, SARS-CoV-2, and delta variant of SARS-CoV-2 by K18-hACE2 mice sera 4 weeks post boost (bleed4). Sera of mice boosted with T2_17 significantly neutralised the Delta variant (B.1.617.2) in comparison to those boosted by AZD1222. The X-axis represents the bleed number, and the Y-axis represents the $\log_{10}IC_{50}$ values for neutralisation curves. **K.** Weight loss profile of K18-hACE2 mice following challenge by the Victoria strain and the Delta variant. All the mice, except naïve were protected. Mann-Whitney U test is used as statistical significance test in all the plots (p-value: * $\leq$0.05, **<0.01, *** $\leq$ 0.001).

To determine the breadth of antibody response and neutralisation in outbred animals, guinea pigs were immunised with T2_17 DNA using the CE approved, and clinically validated Pharmajet Tropis needleless, intradermal delivery device to ensure standardised intradermal

delivery (**Fig. 2A**). As a control we used a C-terminal glycosylation modified SARS-CoV-2 RBD (SARS2_RBD_P521N) (**Fig. 2B**) which we had previously evaluated in BALB/c mice (**Fig. S4**). Generation of neutralising antibodies to both SARS-CoV and SARS-CoV-2 was confirmed using pseudoviruses expressing full-length spike proteins of SARS-CoV, and SARS-CoV-2. While both T2_17 and SARS2_RBD_P521N generated binding antibodies against both SARS-CoV and SARS-CoV-2 (**Fig. 2C**) after one immunisation, T2_17 elicited significantly higher antibodies than SARS2_RBD_P521N to SARS-CoV and comparable antibodies against SARS-CoV-2. Higher binding antibodies were detected for T2_17 to SARS-CoV in comparison to SARS2_RBD_P521N after two immunisations while the responses were comparable for SARS-CoV-2. After three immunisations SARS2_RBD_P521N induced a higher response to SARS-CoV-2, while T2_17 had higher responses to SARS-CoV. Neutralising antibodies were detected for SARS-CoV-2 after first immunisation, while significant neutralising responses to SARS-CoV developed after two immunisations, though more potent for T2_17 than SARS2_RBD_P521N (**Fig. 2D**). Better binding and neutralising responses by SARS2_RBD_P521N to SARS-CoV-2 were expected as it differs from SARS-CoV-2 by only one amino acid. To further confirm, whether T2_17 vaccine design generates broader responses, we compared sera induced by SARS2_RBD_P521N, 28 days post 3rd immunisation for neutralisation against SARS-CoV, WIV16, RaTG13, and SARS-CoV-2. Statistically significant higher titre neutralising antibodies were generated by T2_17 against SARS-CoV, WIV16, and RaTG13 (**Fig. 2E**). To further confirm T2_17 anti-sera could abrogate hACE2 receptor binding, we performed an ELISA based competition assay (**Fig. 2F**) demonstrating T2_17 and SARS2_RBD_P521N anti-sera abrogated binding to hACE-2 receptor and are comparable to the WHO standard of pooled convalescent COVID-19 patient sera. These findings demonstrated important proof-of-concept of T2_17 as a single gene delivered, structurally engineered antigen capable of eliciting broad pan-sarbeco Coronavirus

neutralising antibodies. Prior to clinical trials in humans, a GMP lot of pEVAC T2_17 was manufactured and evaluated for safety and immunogenicity in rabbits using the same gene delivery device to ensure uniform intradermal administration (**Fig. 2G**). After one immunisation, binding antibodies to SARS-CoV and SARS-CoV-2 were elicited (**Fig. 2H**), increasing on subsequent immunisations until a plateau was reached by the fourth immunisation. Robust neutralising antibodies were observed 2 weeks following the third immunisation (**Fig. 2I**) revealing broad neutralising antibody responses against the SARS-CoV, SARS-CoV-2, Beta, Gamma, and Delta VOCs as well as the bat sarbecoviruses – WIV16, and RaTG13 elicited by gene delivery of the engineered T2_17 pan-Sarbeco vaccine antigen candidate (**Fig. 2J**).

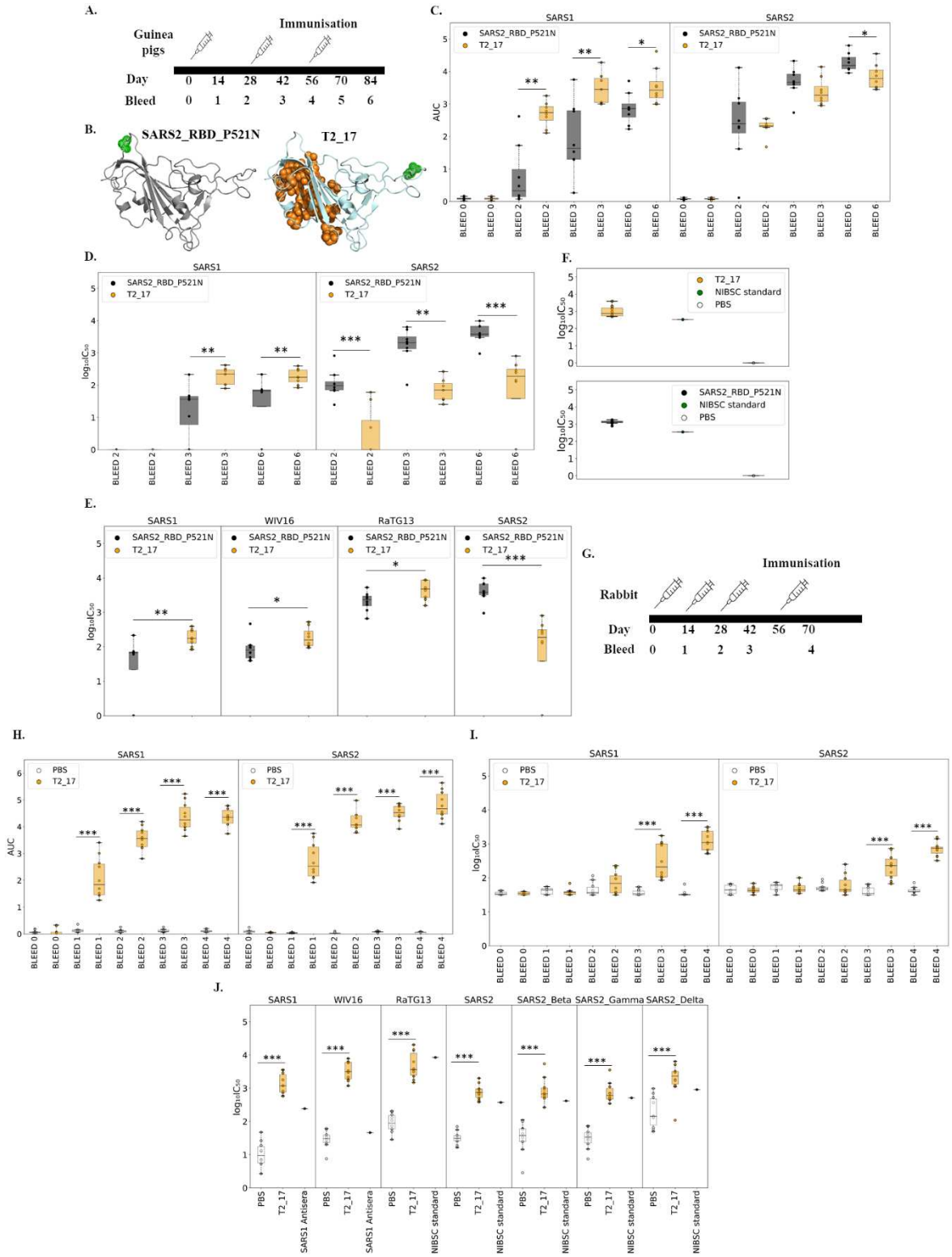

Figure 2| Immunogenicity studies in guinea pigs and rabbits

A. Immunisation and bleed schedule of guinea pigs. Guinea pigs were immunised with DNA delivered intradermally (i.d) by the Tropis ParmaJet device at 28 day intervals and bled every 14 days. **B**. Structure models of the vaccine designs used for the study in guinea pigs. The glycosylation site and the modified epitope are represented as green and orange spheres

respectively. **C.** Elicitation of binding antibodies against SARS-CoV and SARS-CoV-2 by T2_17 and SARS2_RBD_P521N was confirmed using ELISA. T2_17 and SARS2_RBD_P521N generated cross-binding antibodies after one immunisation. The pre-bleed (Bleed 0) is considered as the control for non-specific binding. The X-axis represents the bleed number, and the Y-axis represents the area under the curve (AUC) for ELISA binding curve. **D.** Neutralisation by guinea pig sera immunised with T2_17 and SARS2_RBD_P521N. Both T2_17 and SARS2_RBD_P521N generated neutralising antibodies against SARS-CoV and SARS-CoV-2. The X-axis represents the bleed number, and the Y-axis represents the $log_{10}IC_{50}$ values for neutralisation curves. **E.** Broad-neutralisation of SARS-CoV, WIV16, RaTG13, and SARS-CoV-2 by T2_17 in comparison to SARS2_RBD_P521N. Sera post 28 days after three immunisation (bleed 6) was used for comparison. **F.** ACE-2 competition ELISA. Sera from Guinea pigs immunised with T2_17 and SARS2_RBD_P521N effectively abrogated the interaction of SARS-CoV-2 RBD with ACE-2 receptor. The NIBSC standard (20/162) was used as control. **G.** Immunisation and bleed schedule of Rabbits. Rabbits were immunised at interval of 14 days and bled every 14 days. **H.** Elicitation of binding antibodies against SARS-CoV and SARS-CoV-2 by T2_17 was confirmed using ELISA. T2_17 generated cross-binding antibodies after one immunisation. The X-axis represents the bleed number, and the Y-axis represents the area under the curve (AUC) for ELISA binding curve. **I.** Neutralisation by rabbit sera immunised with T2_17. T2_17 generated neutralising antibodies against SARS-CoV and SARS-CoV-2. The X-axis represents the bleed number, and the Y-axis represents the $log_{10}IC_{50}$ values for neutralisation curves. **J.** Broad-neutralisation of SARS-CoV, WIV16, RaTG13, SARS-CoV-2, SARS-CoV-2 Beta, SARS-CoV-2 Gamma, and SARS-CoV-2 Delta by T2_17. Sera post 14 days after four immunisation (bleed 4) was used for comparison. NISBSC standard for SARS-CoV-2 and SARS-CoV antiserum are used as reference. Mann-Whitney U demonstrated statistical significance (p-value: * $\leq$0.05, **<0.01, *** $\leq$ 0.001).

Emergence of two human epidemics caused by ACE-2 using sarbecoviruses in past two decades highlights the urgent need for vaccines that can provide broad protection from SARS-CoV-2 VOCs as well as to all the ACE-2 receptor using sarbecoviruses that have the potential to spill-over from zoonotic animal reservoirs. To achieve pan-Sarbeco/pan-Beta coronavirus protection, various vaccine strategies have been employed such as mRNA expressing chimeric version of spike proteins from different coronaviruses[26], as well as mosaic and cocktail nanoparticles expressing RBDs of different coronaviruses[27]. Though these strategies have been reported to be effective in generating pan-Sarbeco/pan-Beta coronaviruses immune responses, these require synthesis, manufacturing and formulation of multiple gene constructs. Here, we

describe a new structural informatics platform pipeline for generating a single novel antigen for sarbecoviruses, which generated broader responses to SARS-CoV, SARS-CoV-2 and related bat sarbecoviruses. The informatics platform pipeline generates novel antigens as synthetic genes allowing seamless down-stream immune screening of libraries of broadly reactive vaccine antigens that can be compared and selected for optimal *in vivo* immune responses by nucleic acid delivery. As proof of concept, lead pan-sarbecovirus vaccine antigen candidates were immune selected for the broadest neutralisation profile, as confirmed in 3 species against SARS-CoV, WIV16, RaTG13, SARS-CoV-2 and it's VOCs. Further broadening of vaccine protection across the betacoronavirus genus is being expanded using combinations of multiple, digitally immune optimised antigens selected to immunologically recruit additional T and B effector responses for maximising breadth and depth of immunity to pre-emergent Coronaviruses. This approach is applicable for other complex and variable virus families such as the Influenza viruses which represent current and future pandemic threats.

Acknowledgements
DBPR

References

1. Liu, K. *et al.* Cross-species recognition of SARS-CoV-2 to bat ACE2. *Proc. Natl. Acad. Sci. U. S. A.* **118**, (2021).
2. Olival, K. J. *et al.* Possibility for reverse zoonotic transmission of SARS-CoV-2 to free-ranging wildlife: A case study of bats. *PLOS Pathog.* **16**, e1008758 (2020).
3. Hu, B. *et al.* Discovery of a rich gene pool of bat SARS-related coronaviruses provides new insights into the origin of SARS coronavirus. *PLOS Pathog.* **13**, e1006698 (2017).
4. Menachery, V. D. *et al.* A SARS-like cluster of circulating bat coronaviruses shows potential for human emergence. *Nat. Med.* **21**, 1508–1513 (2015).

5. Vilar, S. & Isom, D. G. One Year of SARS-CoV-2: How Much Has the Virus Changed? *Biology* **10**, (2021).
6. Horspool, A. M. *et al.* SARS-CoV-2 B.1.1.7 and B.1.351 variants of concern induce lethal disease in K18-hACE2 transgenic mice despite convalescent plasma therapy. *BioRxiv Prepr. Serv. Biol.* (2021) doi:10.1101/2021.05.05.442784.
7. Planas, D. *et al.* Sensitivity of infectious SARS-CoV-2 B.1.1.7 and B.1.351 variants to neutralizing antibodies. *Nat. Med.* **27**, 917–924 (2021).
8. Wang, P. *et al.* Increased resistance of SARS-CoV-2 variant P.1 to antibody neutralization. *Cell Host Microbe* **29**, 747-751.e4 (2021).
9. Leung, K., Shum, M. H., Leung, G. M., Lam, T. T. & Wu, J. T. Early transmissibility assessment of the N501Y mutant strains of SARS-CoV-2 in the United Kingdom, October to November 2020. *Euro Surveill. Bull. Eur. Sur Mal. Transm. Eur. Commun. Dis. Bull.* **26**, (2021).
10. Tian, F. *et al.* Mutation N501Y in RBD of Spike Protein Strengthens the Interaction between COVID-19 and its Receptor ACE2. *bioRxiv* 2021.02.14.431117 (2021) doi:10.1101/2021.02.14.431117.
11. Campbell, F. *et al.* Increased transmissibility and global spread of SARS-CoV-2 variants of concern as at June 2021. *Eurosurveillance* **26**, 2100509 (2021).
12. Wu, Y. *et al.* A noncompeting pair of human neutralizing antibodies block COVID-19 virus binding to its receptor ACE2. *Science* **368**, 1274–1278 (2020).
13. Hwang, W. C. *et al.* Structural Basis of Neutralization by a Human Anti-severe Acute Respiratory Syndrome Spike Protein Antibody, 80R. *J. Biol. Chem.* **281**, 34610–34616 (2006).
14. Pinto, D. *et al.* Cross-neutralization of SARS-CoV-2 by a human monoclonal SARS-CoV antibody. *Nature* **583**, 290–295 (2020).

15. Yuan, M. *et al.* A highly conserved cryptic epitope in the receptor binding domains of SARS-CoV-2 and SARS-CoV. *Science* **368**, 630–633 (2020).
16. Hatcher, E. L. *et al.* Virus Variation Resource - improved response to emergent viral outbreaks. *Nucleic Acids Res.* **45**, D482–D490 (2017).
17. Li, W. *et al.* Animal Origins of the Severe Acute Respiratory Syndrome Coronavirus: Insight from ACE2-S-Protein Interactions. *J. Virol.* **80**, 4211–4219 (2006).
18. Lavie, M., Hanoulle, X. & Dubuisson, J. Glycan Shielding and Modulation of Hepatitis C Virus Neutralizing Antibodies. *Front. Immunol.* **9**, 910 (2018).
19. Watanabe, Y. *et al.* Structure of the Lassa virus glycan shield provides a model for immunological resistance. *Proc. Natl. Acad. Sci. U. S. A.* **115**, 7320–7325 (2018).
20. Eggink, D., Goff, P. H. & Palese, P. Guiding the immune response against influenza virus hemagglutinin toward the conserved stalk domain by hyperglycosylation of the globular head domain. *J. Virol.* **88**, 699–704 (2014).
21. Schymkowitz, J. *et al.* The FoldX web server: an online force field. *Nucleic Acids Res.* **33**, W382–W388 (2005).
22. Nguyen, L.-T., Schmidt, H. A., von Haeseler, A. & Minh, B. Q. IQ-TREE: A Fast and Effective Stochastic Algorithm for Estimating Maximum-Likelihood Phylogenies. *Mol. Biol. Evol.* **32**, 268–274 (2015).
23. Ashkenazy, H. *et al.* ConSurf 2016: an improved methodology to estimate and visualize evolutionary conservation in macromolecules. *Nucleic Acids Res.* **44**, W344–W350 (2016).
24. Schrödinger, L. & DeLano, W. *PyMOL*. (2020).
25. Berman, H. M. *et al.* The Protein Data Bank. *Nucleic Acids Res.* **28**, 235–242 (2000).

26. Martinez, D. R. *et al.* Chimeric spike mRNA vaccines protect against Sarbecovirus challenge in mice. *BioRxiv Prepr. Serv. Biol.* 2021.03.11.434872 (2021) doi:10.1101/2021.03.11.434872.

27. Walls, A. C. *et al.* Elicitation of broadly protective sarbecovirus immunity by receptor-binding domain nanoparticle vaccines. *Cell* (2021) doi:10.1016/j.cell.2021.09.015.

Methods

Phylogenetic analysis

Protein sequences of spike proteins were downloaded from the NCBI virus database for all the known sarbecoviruses. A multiple sequence alignment (MSA) was generated usingMUSCLE[1]. The resulting MSA was pruned to the RBD region and used as input for phylogenetic tree reconstruction. The phylogenetic tree was generated using IQTREE [2] using the protein model with the best BIC score. The resultant tree was used for generation of phylogenetically optimised design using HyPhy[3].

Epitope identification

Available structural data for spike protein-antibody complexes for SARS-CoV and SARS-CoV-2 were downloaded from the Protein Databank (PDB)[4]. Structural data were then pruned for antigen-antibody complexes where the epitopes were on the RBD. Amino acid residues of antigen that have at least one atom within 5Å radii of at least one atom of amino acid of antibody were defined as epitope residues,with epitope regions defined as contiguous stretches of at least 5 amino acids.

Molecular modelling

Structural models were generated for T2_13 using MODELLER[5,6] using both SARS-CoV and SARS-CoV-2 structures as templates. The structural model with the highest DOPE score[7] was chosen as the working model for further molecular modelling. The side chains for the model were further optimised using SCWRL[8] and energy minimised using GROMACS [9]. For T2-14 to T2-18, mutations were introduced using T2-13 as the reference structure using BUILD module of FOLDX algorithm[10] and checked for structural stability using FOLDX forcefield[10].

Production and transformation of plasmids.

Sequences of vaccine designs were gene-optimized and adapted to human codon use via the GeneOptimizer algorithm[11]. These genes were cloned into pEVAC (GeneArt, Germany) via restriction digestion. Plasmids were transformed via heat-shock in chemically induced competent *E. coli* DH5α cells (Invitrogen 18265-017). Plasmid DNA was extracted from transformed bacterial cultures via the Plasmid Mini Kit (Qiagen 12125). All plasmids were subsequently quantified using UV spectrophotometry (NanoDrop™ -Thermo Scientific).

Vaccination Experiments in Mice.

Eleven groups of six female 8–10-week-old BALB/c mice were purchased from Charles River Laboratories (Kent, United Kingdom). Mice were immunised a total of four times with 30 days intervals. A total volume of 50µl of PBS containing 50µg of plasmid DNA was administered via subcutaneous route in the rear flank. Blood was sampled from the saphenous vein at 15 days intervals, and animals were terminally bled by cardiac puncture under non-recovery anaesthesia at day 150.

Fluorescence assisted cell sorting (FACS) assay

HEK293T cells were transfected with an expression plasmid expressing wild-type spike glycoprotein of each of the four ACE-2 binding sarbecoviruses *including* SARS-CoV, SARS--CoV-2, RaTG13, and WIV16. 48 hours after transfection, cells were transferred into V-bottom 96-well plates (50,000 cells/well). Cells were incubated with sera (diluted at 1:50 in PBS) or anti-mouse IgG Isotype negative control (Invitrogen 10400C, diluted at 20µg/mL in PBS) for 30 min, washed with FACS buffer (PBS, 1% FBS, 0.02% Tween 20) and stained with Goat anti-mouse IgG (H+L) Alexa Fluor 647 Secondary Antibody (Invitrogen A32728, diluted at 20µg/mL in FACS buffer), for 30 min in the dark. Cells were washed with FACS buffer and samples were run on a Attune NxT Flow Cytometer (Invitrogen) with a high-throughput auto sampler. Dead cells were excluded from the analysis by staining cells with 7-Aminoactinomycin D (7-AAD) and gating 7-AAD negative live cells.

Enzyme-linked immunosorbent assay (ELISA)

The assays were adapted from those originally described by Amanat and co-workers[12]. Briefly, Nunc MaxiSorp™ flat-bottom plates were coated with 50µl per well of 1µg/ml of RBD from SARS-1 or SARS-2 DPBS (-Ca^{2+}/-Mg^{2+}) and incubated overnight at 4°C. The next day, the plates were blocked with 3% milk in PBST (0.1% w/v Tween20 in PBS) for 1 hour. After removing the blocking buffer, 50µl/well of serum samples diluted in PBST-NFM (1% w/w non-fat milk in PBST) were added to the plates and incubated on a plate shaker for two hours at 20°C. The plates were washed three times with 200µl of PBST, and then 50µl of HRP-conjugated goat anti Ig (H and L chains) (Jackson ImmunoResearch) was added to each well and left to incubate for one hour on a plate shaker for 1 hour. Plates were washed three times with 200µl of PBST, 50µl/well of 1-Step Ultra TMB chromogenic substrate (Sigma) was added to the plates and the chemical reaction was stopped three minutes later with 50µl 2N H_2SO_4.

The optical density at a wavelength of 450nm (OD450) was measured using a BioRad microplate reader. Values from the dilution curve were used to determine the area under the curve.

Pseudotype-based micro-neutralisation assay

Pseudotype-based micro-neutralisation assay was performed as described previously[13]. Briefly, serial dilutions of serum were incubated with SARS-CoV-2/RaTG13/SARS-CoV/WIV16 spike bearing lentiviral pseudotypes for 1 h at 37°C, 5% CO_2 in 96-well white cell culture plates. $1.5x10^4$ HEK293T/17 transiently expressing human ACE-2 and TMPRSS2 were then added per well and plates incubated for 48 hrs at 37°C, 5% CO_2 in a humidified incubator. Bright-Glo (Promega) was then added to each well and luminescence read after a five-minute incubation period. Experimental data points were normalised to 100% and 0% neutralisation controls and non-linear regression analysis performed in GraphPad Prism 9 to produce neutralisation curves and IC_{50} values.

Vaccine boost efficacy studies in K18-hACE2 mice.

Ten groups of six female 8–15-week-old homozygous K18-hACE2 mice (Jax) were primed with $1.4x10^9$ viral particles of AZD1222 or PBS by intramuscular route, in a total volume of 100µl split over the two rear legs. After 28 days, two groups of six mice were boosted with PBS, AZD1222, or T2_17 DNA. Mice were bled at two-week intervals and challenged at day 84 with either Victoria/1/2020 (B-type) or Delta SARS-CoV-2 by intranasal route, in a total volume of 40µl over both nares. Mice were weighed daily and monitored for clinical signs for a period of 10 days before being culled by terminal bleed.

Intradermal nucleic acid immunisation with Tropis PharmaJet delivery in Guinea pigs.

Two groups of eight female 7-week-old Dunkin Hartley Guinea pigs (Envigo RMS, Blackthorn, United Kingdom) were immunised a total of three times with 28 days intervals. A total volume of 200µl of PBS containing 400µg of plasmid DNA was administered by PharmaJet Tropis intradermal device, split over each hind leg. Blood was sampled from the saphenous vein at 14 days intervals.

Intradermal nucleic acid immunisation with Tropis PharmaJet delivery in in Rabbits.

Ten mature (five male, five female) rabbits were immunised with a GMP lot pEVAC_T2_17 (clinical pEVAC_PS) intradermally by PharmaJet Tropis needleless delivery to the upper left and right hind limbs (300µl at 2mg/mL). For control group, ten mature (five male, five female) rabbits were injected with PBS. Arterial blood was sampled at 14 days intervals

ACE-2 competition assay

The SARS-CoV-2 surrogate virus neutralisation test (SVNT, Genscript, Piscataway, New Jersey, United States) was carried out as per manufacturer's instructions. Briefly, serum from bleed 6 guinea pigs were diluted in PBS across an 8 point 1:2 dilution series from a starting concentration of 1:50. Samples were further diluted in the provided sample buffer at a 1:9 ratio, and then mixed with HRP conjugated to SARS-CoV-2 RBD protein, incubated at 37°C for 30 min and added to human ACE-2 protein coated wells in 96-well plate format. The reaction was incubated at 37°C for 15 min and then washed four times with provided wash buffer. TMB solution was then added, incubated for 15 minutes in the dark at R.T to allow the reaction to develop. The reaction was then quenched using the provided stop solution, and then absorbance read at 450 nm.

Statistical analyses

Mann-Whitney U tests were performed for all the comparisons using the Python sklearn package[14]. All the plots were generated using the Python Matplotlib package[15].

References

1. Edgar, R. C. MUSCLE: a multiple sequence alignment method with reduced time and space complexity. *BMC Bioinformatics* **5**, 113 (2004).
2. Nguyen, L.-T., Schmidt, H. A., von Haeseler, A. & Minh, B. Q. IQ-TREE: A Fast and Effective Stochastic Algorithm for Estimating Maximum-Likelihood Phylogenies. *Mol. Biol. Evol.* **32**, 268–274 (2015).
3. Pond, S. L. K., Frost, S. D. W. & Muse, S. V. HyPhy: hypothesis testing using phylogenies. *Bioinformatics* **21**, 676–679 (2005).
4. Berman, H. M. *et al.* The Protein Data Bank. *Nucleic Acids Res.* **28**, 235–242 (2000).
5. Eswar, N. *et al.* Comparative protein structure modeling using MODELLER. *Curr. Protoc. Protein Sci.* **Chapter 2**, Unit 2.9 (2007).
6. Sali, A. & Blundell, T. L. Comparative protein modelling by satisfaction of spatial restraints. *J. Mol. Biol.* **234**, 779–815 (1993).
7. Shen, M. & Sali, A. Statistical potential for assessment and prediction of protein structures. *Protein Sci. Publ. Protein Soc.* **15**, 2507–2524 (2006).
8. Krivov, G. G., Shapovalov, M. V. & Dunbrack, R. L. Improved prediction of protein side-chain conformations with SCWRL4: Side-Chain Prediction with SCWRL4. *Proteins Struct. Funct. Bioinforma.* **77**, 778–795 (2009).
9. Van Der Spoel, D. *et al.* GROMACS: fast, flexible, and free. *J. Comput. Chem.* **26**, 1701–1718 (2005).

10. Schymkowitz, J. *et al.* The FoldX web server: an online force field. *Nucleic Acids Res.* **33**, W382–W388 (2005).

11. Raab, D., Graf, M., Notka, F., Schödl, T. & Wagner, R. The GeneOptimizer Algorithm: using a sliding window approach to cope with the vast sequence space in multiparameter DNA sequence optimization. *Syst. Synth. Biol.* **4**, 215–225 (2010).

12. Amanat, F. *et al.* A serological assay to detect SARS-CoV-2 seroconversion in humans. *Nat. Med.* **26**, 1033–1036 (2020).

13. Carnell, G., Grehan, K., Ferrara, F., Molesti, E. & Temperton, N. J. An Optimised Method for the Production using PEI, Titration and Neutralization of SARS-CoV Spike Luciferase Pseudotypes. *Bio-Protoc.* **7**, (2017).

14. Pedregosa, F. *et al.* Scikit-learn: Machine Learning in Python. *J. Mach. Learn. Res.* **12**, 2825–2830 (2011).

15. Hunter, J. D. Matplotlib: A 2D Graphics Environment. *Comput. Sci. Eng.* **9**, 90–95 (2007).

Supplementary Files

This is a list of supplementary files associated with this preprint. Click to download.

- 20210914222T217supplfinal260921.pdf
- rs.pdf